Advances in Applied Mathematics and Mechanics
Adv. Appl. Math. Mech., Vol. **xx**, No. x, pp. 1-17

DOI: 10.4208/aamm.OA-2022-0182
xxx 2024

Superconvergence Error Estimate of the Bilinear-Constant Scheme for the Stokes Equations with Damping

Huaijun Yang*, Lele Wang and Xin Liao

School of Mathematics, Zhengzhou University of Aeronautics, Zhengzhou, Henan 450046, China

Received 7 July 2022; Accepted (in revised version) 28 February 2023

Abstract. In this paper, the superconvergence error estimate of a low-order conforming mixed finite element scheme, which is called bilinear-constant scheme, for the Stokes equations with damping is established. In terms of the integral identity technique and dealing with the damping term carefully, the superclose estimates between the interpolation of the exact solution and the finite element solution for the velocity in H^1-norm and the pressure in L^2-norm are first derived. Then, the global superconvergence results for the velocity in H^1-norm and the pressure in L^2-norm are derived by a simple postprocessing technique with an economical workload. Finally, some numerical results are presented to demonstrate the correctness of the theoretical analysis.

AMS subject classifications: 65M15, 65M60, 65N12

Key words: Stokes equations with damping, bilinear-constant scheme, superclose and superconvergence estimates.

1 Introduction

This paper focus on the superconvergence error estimate with a low-order conforming mixed finite element method for the following stationary Stokes equations with damping:

$$\begin{cases} -\nu\Delta \boldsymbol{u}+\alpha|\boldsymbol{u}|^{r-2}\boldsymbol{u}+\nabla p=\boldsymbol{f}, & \boldsymbol{x}\in\Omega, \\ \nabla\cdot\boldsymbol{u}=0, & \boldsymbol{x}\in\Omega, \\ \boldsymbol{u}=0, & \boldsymbol{x}\in\partial\Omega, \end{cases} \tag{1.1}$$

where $\Omega\subset\mathbb{R}^2$ is a rectangular domain with boundary $\partial\Omega$ and $\boldsymbol{x}=(x,y)$. $\boldsymbol{u}=(u_1,u_2)$ is the fluid velocity, p is the pressure and $\boldsymbol{f}$ is a given external force, respectively. The parameter ν is the viscosity and $|\cdot|$ denotes the Euclidean norm. Moreover, the Forchheimer (or

*Corresponding author.
Emails: huaijunyang@zua.edu.cn (H. Yang), wanglesky@163.com (L. Wang), woshiliaoxin@126.com (X. Liao)

damping) term $\alpha|\boldsymbol{u}|^{r-2}\boldsymbol{u}$ with coefficient $\alpha>0$ and $2\le r<\infty$ comes from Forchheimer's law [1], which describes various physical situations such as porous media flow, drag, or friction effects and some dissipative mechanisms [2,3].

The mathematical analysis and numerical approximation of (1.1) have attracted considerable interests. The existence and uniqueness of the weak solution and the discrete solution were proven in [4], and the corresponding optimal error estimates were obtained for conforming mixed finite element methods. In [5], a local projection stablization method was used to overcome the lack of the inf-sup condition with low order mixed finite element spaces, and optimal error estimates for the velocity and the pressure were derived. The mark and cell method was applied to discretize (1.1) on the non-uniform grids, and the stability and the error estimates were studied in [6]. In addition, in [7], a class of conforming finite element methods were employed to (1.1) and the superclose and superconvergence for the velocity in H^1-norm and the pressure in L^2-norm were obtained with some restrictions on ν due to estimate the damping term roughly. Meanwhile, the degrees of freedom is larger than the bilinear-constant scheme presented in this paper. Moreover, we refer the readers to [8–10] for the Navier-Stokes equations with damping.

On the other hand, it is well known that superconvergence is an efficient procedure for improving the accuracy of the approximation solutions in numerical analysis [11,12]. We refer the readers to [13–23] and the references cited therein for the superconvergence analysis for different problems. Especially, the supeconvergence analysis was investigated for Stokes and Navier-Stokes equations by low order nonconforming finite element method in [22] and [23], respectively. In addition, the superconvergence analysis was studied by a stable conforming bilinear-constant scheme for Stokes equations over a uniform rectangular mesh in [24]. The bilinear-constant scheme was also applied to optimal control problems governed by Stokes equations and the global superconvergence analysis for the finite element approximation was discussed in [25]. Compared with Navier-Stokes equations, Stokes equations with damping are more complicated for the nonlinear damping term $\alpha|\boldsymbol{u}|^{r-2}\boldsymbol{u}$, while Navier-Stokes equations have a linear damping term.

This paper studies the superconvergence property by the bilinear-constant scheme used in [24,25] for the Stokes equations with damping over a uniform rectangular mesh. The superclose error estimates between the interpolation of the exact solution and the finite element solution are first derived by the integral identity technique [11,12,24,25] and dealing with the damping term carefully. Then, the global superconvergence results are obtained by a postprocessing technique. Finally, some numerical results are presented to verify the theoretical findings.

The outline of this paper is as follows. In Section 2, we introduce some preliminaries and recall some lemmas, which are necessary in the following error estimates. In Section 3, we present the detailed superclose and superconvergence error analysis for problem (1.1). In Section 4, we provide some numerical results to verify the theoretical analysis. Some conclusions are given in the final section.

2 Preliminaries

We will use standard notations for the Sobolev spaces $H^m(\Omega)$, $m\geq 0$ (cf. [26]) with the norm $\|\cdot\|_m$ and seminorm $|\cdot|_m$. In the case $m=0$, then $H^0(\Omega)=L^2(\Omega)$, the norm and inner product are denoted by $\|\cdot\|_0$ and $(\cdot,\cdot)$, respectively.

The weak formulation of (1.1) is: to seek $(\boldsymbol{u},p)\in(H_0^1(\Omega))^2\times L_0^2(\Omega)$ such that

$$
\begin{aligned}
&a(\boldsymbol{u};\boldsymbol{u},\boldsymbol{v})-b(\boldsymbol{v},p)=(\boldsymbol{f},\boldsymbol{v}), && \forall \boldsymbol{v}\in(H_0^1(\Omega))^2, && (2.1a)\\
&b(\boldsymbol{u},q)=0, && \forall q\in L_0^2(\Omega), && (2.1b)
\end{aligned}
$$

where

$$
\begin{aligned}
&a_0(\boldsymbol{u},\boldsymbol{v})=\nu(\nabla\boldsymbol{u},\nabla\boldsymbol{v}), \qquad a_1(\boldsymbol{u};\boldsymbol{u},\boldsymbol{v})=\alpha(|\boldsymbol{u}|^{r-2}\boldsymbol{u},\boldsymbol{v}),\\
&a(\boldsymbol{u};\boldsymbol{u},\boldsymbol{v})=a_0(\boldsymbol{u},\boldsymbol{v})+a_1(\boldsymbol{u};\boldsymbol{u},\boldsymbol{v}),\\
&b(\boldsymbol{v},p)=(p,\nabla\cdot\boldsymbol{v}),\\
&H_0^1(\Omega)=\{w\in H^1(\Omega):\ w|_{\partial\Omega}=0\},\quad L_0^2(\Omega)=\left\{q\in L^2(\Omega):\ \int_\Omega q\,dxdy=0\right\}.
\end{aligned}
$$

Let $\mathcal{T}_h=\{e\}$ be a uniform rectangular mesh over Ω with mesh-size h. For a given element $e\in\mathcal{T}_h$, its four vertices are denoted by $a_i(x_i,y_i)$, $i=1,2,3,4$ in the counterclockwise order (see Fig. 1(a)). For the velocity, we choose $\boldsymbol{X}_h$ as the general bilinear finite element space. For the pressure, we assume that the subdivision $\mathcal{T}_h$ is obtained from $\mathcal{T}_{2h}=\{\tau\}$ by dividing each element of $\mathcal{T}_{2h}$ into four small congruent rectangles. Let $P_h^{'}$ consist of piecewise constant functions with respect to $\mathcal{T}_h$ such that the local basis functions for $P_h^{'}$ on a 2×2-patch of τ (see Fig. 1(b)) are indicated in Fig. 2. Then, the finite element space for pressure is defined by $P_h^{'}\cap L_0^2(\Omega)$. In the following discussion we always assume that $\tau=\cup_{i=1}^4 e_i\in\mathcal{T}_{2h}$ with $e_i\in\mathcal{T}_h$ $(1\leq i\leq 4)$ (see Fig. 1(b)). Thus, the finite element approximation

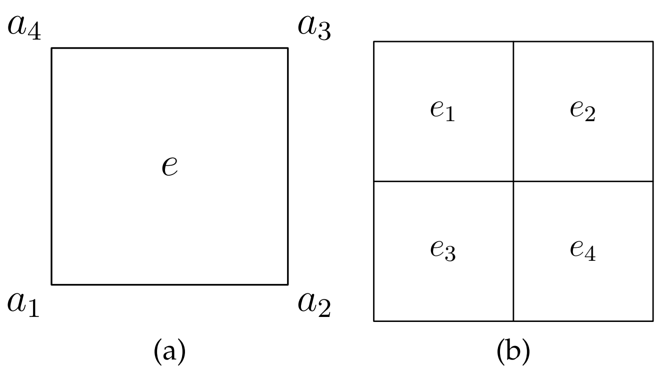

Figure 1: The element e (a) and τ (b).

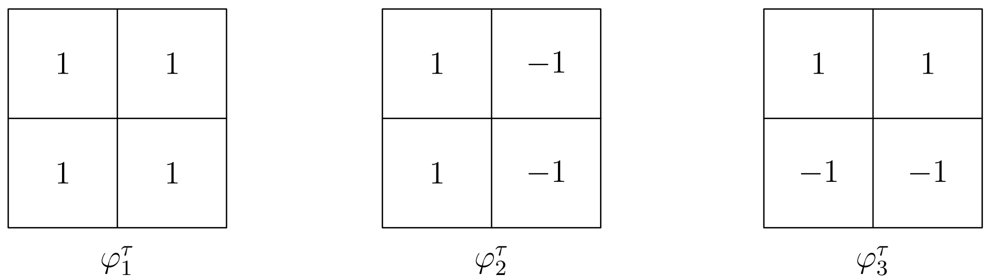

Figure 2: Local basis functions of P_h'.

spaces $\boldsymbol{X}_h$ and P_h for the bilinear-constant scheme are described by (cf. [24,27])

$$\boldsymbol{X}_h = \{\boldsymbol{v} \in (C(\overline{\Omega}))^2 : \boldsymbol{v}|_e \in (Q_{11}(e))^2, \boldsymbol{v}|_{\partial\Omega} = 0, e \in \mathcal{T}_h\},$$
$$P_h = \left\{ p \in L_0^2(\Omega) : p|_\tau = \sum_{i=1}^{3} \lambda_i^\tau \varphi_i^\tau, \sum_{\tau \in \mathcal{T}_{2h}} \lambda_1^\tau = 0, \tau \in \mathcal{T}_{2h} \right\},$$

where Q_{11} denotes the space of all polynomials of degree ≤ 1 with respect to each of the two variables x and y and $\lambda_i^T \in \mathbb{R}$.

It has been shown in [24,27] that the bilinear-constant scheme satisfies the Babuška-Brezzi condition, i.e.,

$$\sup_{0 \neq \boldsymbol{v}_h \in \boldsymbol{X}_h} \frac{(q_h, \nabla \cdot \boldsymbol{v}_h)}{\|\boldsymbol{v}_h\|_1} \geq \beta \|q_h\|_0, \quad \forall q_h \in P_h, \tag{2.2}$$

where $\beta > 0$ is a constant independent of h.

Now, we are in the position to present the bilinear-constant finite element approximation of (2.1a)-(2.1b) as follows: find $(\boldsymbol{u}_h, p_h) \in \boldsymbol{X}_h \times P_h$, such that

$$a(\boldsymbol{u}_h; \boldsymbol{u}_h, \boldsymbol{v}_h) - b(\boldsymbol{v}_h, p_h) = (\boldsymbol{f}, \boldsymbol{v}_h), \qquad \forall \boldsymbol{v}_h \in \boldsymbol{X}_h, \tag{2.3}$$
$$b(\boldsymbol{u}_h, q_h) = 0, \qquad \forall q_h \in P_h. \tag{2.4}$$

To present the error estimate, let $\boldsymbol{V}_h = \{\boldsymbol{v}_h \in \boldsymbol{X}_h : (\nabla \cdot \boldsymbol{v}_h, \mu_h) = 0, \forall \mu_h \in P_h\}$ and define the following problem: find $\boldsymbol{u}_h \in \boldsymbol{V}_h$ such that

$$a(\boldsymbol{u}_h; \boldsymbol{u}_h, \boldsymbol{v}_h) = (\boldsymbol{f}, \boldsymbol{v}_h), \quad \forall \boldsymbol{v}_h \in \boldsymbol{V}_h. \tag{2.5}$$

The existence and uniqueness of (2.3)-(2.4) and (2.5) has been proved in [4].

Moreover, for $\boldsymbol{u}_h \in \boldsymbol{V}_h$, there hold the following prior estimates [4]:

$$\|\boldsymbol{u}_h\|_1 \leq \frac{\|\boldsymbol{f}\|_{-1}}{\nu}, \quad \|\boldsymbol{u}_h\|_{0,r} \leq 2\sqrt[r]{\frac{\|\boldsymbol{f}\|_{-1}^2}{\alpha\nu}}. \tag{2.6}$$

Let $\mathcal{I}_h:(C(\overline{\Omega}))^2\rightarrow \boldsymbol{V}_h$ be the Lagrange interpolation operator for the velocity, i.e.,

$$\mathcal{I}_h\boldsymbol{v}(a_i)=\boldsymbol{v}(a_i),\quad i=1,2,3,4,\quad \forall \boldsymbol{v}\in (H^2(\Omega))^2.$$

For the pressure, we first introduce the local L^2-project $\mathcal{J}_h^{'}p$ of p by

$$\mathcal{J}_h^{'}p|_e=\frac{1}{|e|}\int_e pdxdy,\quad \forall e\in\mathcal{T}_h.$$

Next, we define the operator $\mathcal{J}_h$ with respect to τ by

$$\mathcal{J}_hp|_{e_i}=\begin{cases} \mathcal{J}_h^{'}p-\dfrac{1}{4}\alpha_\tau, & i=1,4,\\ \mathcal{J}_h^{'}p+\dfrac{1}{4}\alpha_\tau, & i=2,3,\end{cases}$$

where $\alpha_\tau=p_1^\tau-p_2^\tau-p_3^\tau+p_4^\tau$ with the notations of

$$p_i^\tau=\frac{1}{|e_i|}\int_{e_i}pdxdy$$

and e_i $(i=1,2,3,4)$ are small elements in τ (see Fig. 1). A direction calculation shows that

$$\mathcal{J}_hp|_\tau=\frac{1}{4}\left[\left(\sum_{i=1}^4 p_i^\tau\varphi_1^\tau\right)+(p_1^\tau-p_2^\tau+p_3^\tau-p_4^\tau)\varphi_2^\tau+(p_1^\tau+p_2^\tau-p_3^\tau-p_4^\tau)\varphi_3^\tau\right],$$

which implies that $\mathcal{J}_hp\in P_h$ for $p\in L_0^2(\Omega)$.

From [24], we have the following lemmas obtained from integral identity technique, which play a key role in the superclose and superconvergence error analysis.

Lemma 2.1. *Suppose that $\boldsymbol{u}\in(H^3(\Omega))^2$, we have*

$$(\nabla(\boldsymbol{u}-\mathcal{I}_h\boldsymbol{u}),\nabla\boldsymbol{v}_h)\le Ch^2\|\boldsymbol{u}\|_3\|\nabla\boldsymbol{v}_h\|_0,\qquad \forall\boldsymbol{v}_h\in\boldsymbol{X}_h,\tag{2.7a}$$

$$(q_h,\nabla\cdot(\boldsymbol{u}-\mathcal{I}_h\boldsymbol{u}))\le Ch^2\|\boldsymbol{u}\|_3\|q_h\|_0,\qquad \forall q_h\in P_h.\tag{2.7b}$$

Lemma 2.2. *Suppose that $p\in H^2(\Omega)$, we have*

$$(p-\mathcal{J}_hp,\nabla\cdot\boldsymbol{v}_h)\le Ch^2\|p\|_2\|\nabla\boldsymbol{v}_h\|_0,\quad \forall\boldsymbol{v}\in\boldsymbol{X}_h.\tag{2.8}$$

3 The superclose and superconvergence error estimates of the bilinear-constant scheme

We first present the superclose error estimate in the following theorem.

Theorem 3.1. *Suppose that* $(\boldsymbol{u},p) \in (H^3(\Omega)\cap H_0^1(\Omega))^2 \times H^2(\Omega)\cap L_0^2(\Omega)$ *be the solution of* (2.1a)-(2.1b) *and* $(\boldsymbol{u}_h,p_h)\in \boldsymbol{X}_h \times P_h$ *be the solution of* (2.3)-(2.4)*, respectively. Then, we have*

$$\|\boldsymbol{u}_h-\mathcal{I}_h\boldsymbol{u}\|_1+\|p_h-\mathcal{J}_hp\|_0\le Ch^2. \tag{3.1}$$

Proof. For simplicity, we split the following error functions as

$$\begin{aligned}
\boldsymbol{u}-\boldsymbol{u}_h&=\boldsymbol{u}-\mathcal{I}_h\boldsymbol{u}+\mathcal{I}_h\boldsymbol{u}-\boldsymbol{u}_h:=\boldsymbol{\sigma}+\boldsymbol{\theta},\\
p-p_h&=p-\mathcal{J}_hp+\mathcal{J}_hp-p_h:=\xi+\eta.
\end{aligned}$$

From (2.1a)-(2.1b) and (2.3)-(2.4), we have

$$\nu(\nabla(\boldsymbol{u}-\boldsymbol{u}_h),\nabla \boldsymbol{v}_h)+\alpha(|\boldsymbol{u}|^{r-2}\boldsymbol{u}-|\boldsymbol{u}_h|^{r-2}\boldsymbol{u}_h,\boldsymbol{v}_h)-(p-p_h,\nabla\cdot \boldsymbol{v}_h)=0, \tag{3.2a}$$
$$(\nabla\cdot(\boldsymbol{u}-\boldsymbol{u}_h),q_h)=0. \tag{3.2b}$$

Then, let $\boldsymbol{v}_h=\boldsymbol{\theta}=\mathcal{I}_h\boldsymbol{u}-\boldsymbol{u}_h$ and $q_h=\eta=\mathcal{J}_hp-p_h$, it follows from (3.2a)-(3.2b) that

$$\begin{aligned}
\nu\|\nabla\boldsymbol{\theta}\|_0^2=&-\nu(\nabla(\boldsymbol{u}-\mathcal{I}_h\boldsymbol{u}),\nabla\boldsymbol{\theta})-\alpha(|\boldsymbol{u}|^{r-2}\boldsymbol{u}-|\boldsymbol{u}_h|^{r-2}\boldsymbol{u}_h,\boldsymbol{\theta})\\
&+(p-\mathcal{J}_hp,\nabla\cdot\boldsymbol{\theta})-(\nabla\cdot(\boldsymbol{u}-\mathcal{I}_h\boldsymbol{u}),\eta):=\sum_{i=1}^4E_i.
\end{aligned} \tag{3.3}$$

By Lemmas 2.1 and 2.2, we have

$$E_1\le Ch^2\|\boldsymbol{u}\|_3\|\nabla\boldsymbol{\theta}\|_0, \tag{3.4a}$$
$$E_3\le Ch^2\|p\|_2\|\nabla\boldsymbol{\theta}\|_0, \tag{3.4b}$$
$$E_4\le Ch^2\|\boldsymbol{u}\|_3\|\eta\|_0. \tag{3.4c}$$

To estimate E_2, we split it into:

$$E_2=-\alpha(|\boldsymbol{u}|^{r-2}\boldsymbol{u}-|\mathcal{I}_h\boldsymbol{u}|^{r-2}\mathcal{I}_h\boldsymbol{u},\boldsymbol{\theta})-\alpha(|\mathcal{I}_h\boldsymbol{u}|^{r-2}\mathcal{I}_h\boldsymbol{u}-|\boldsymbol{u}_h|^{r-2}\boldsymbol{u}_h,\boldsymbol{\theta}):=E_{21}+E_{22}.$$

From the following inequality (cf. [5])

$$\big||\boldsymbol{a}|^{r-2}\boldsymbol{a}-|\boldsymbol{b}|^{r-2}\boldsymbol{b}\big|\le C(|\boldsymbol{a}|+|\boldsymbol{b}|)^{r-2}|\boldsymbol{a}-\boldsymbol{b}|,\quad \forall \boldsymbol{a},\boldsymbol{b}\in\mathbb{R}^2,\quad C>0,$$

we have by Holder inequality and Minkowski inequality

$$\begin{aligned}
E_{21}\le&\alpha\int_\Omega\big||\boldsymbol{u}|^{r-2}\boldsymbol{u}-|\mathcal{I}_h\boldsymbol{u}|^{r-2}\mathcal{I}_h\boldsymbol{u}\big||\boldsymbol{\theta}|dxdy\\
\le&\alpha C\int_\Omega(|\boldsymbol{u}|+|\mathcal{I}_h\boldsymbol{u}|)^{r-2}|\boldsymbol{u}-\mathcal{I}_h\boldsymbol{u}||\boldsymbol{\theta}|dxdy\\
\le&\alpha C\left(\int_\Omega\left[(|\boldsymbol{u}|+|\mathcal{I}_h\boldsymbol{u}|)^{r-2}\right]^{r'}dxdy\right)^{\frac{1}{r'}}\left(\int_\Omega|\boldsymbol{u}-\mathcal{I}_h\boldsymbol{u}|^r dxdy\right)^{\frac{1}{r}}\left(\int_\Omega|\boldsymbol{\theta}|^r dxdy\right)^{\frac{1}{r}}\\
\le&\alpha C(\|\boldsymbol{u}\|_{0,r}+\|\mathcal{I}_h\boldsymbol{u}\|_{0,r})^{r-2}\|\boldsymbol{u}-\mathcal{I}_h\boldsymbol{u}\|_{0,r}\|\boldsymbol{\theta}\|_{0,r},
\end{aligned} \tag{3.5}$$

where $\frac{1}{r'}+\frac{2}{r}=1$.

Furthermore, according to interpolate theory and Sobolev imbedding theorem [28], one can check that

$$\begin{aligned}&\|\boldsymbol{u}-\mathcal{I}_h\boldsymbol{u}\|_{0,r}\le Ch^2\|\boldsymbol{u}\|_{2,r}\le Ch^2\|\boldsymbol{u}\|_3,\\&\|\mathcal{I}_h\boldsymbol{u}-\boldsymbol{u}_h\|_{0,r}\le C\|\nabla(\mathcal{I}_h\boldsymbol{u}-\boldsymbol{u}_h)\|_0.\end{aligned}$$

Thus, E_{21} reduces to

$$E_{21}\le\alpha Ch^2(\|\boldsymbol{u}\|_{0,r}+\|\mathcal{I}_h\boldsymbol{u}\|_{0,r})^{r-2}\|\boldsymbol{u}\|_3\|\nabla\boldsymbol{\theta}\|_0\le Ch^2\|\nabla\boldsymbol{\theta}\|_0. \tag{3.6}$$

Moreover, by Tartar inequality, i.e., $\forall\boldsymbol{a},\ \boldsymbol{b}\in\mathbb{R}^2$ and $s\ge 0$, there holds

$$(\boldsymbol{a}|\boldsymbol{a}|^s-\boldsymbol{b}|\boldsymbol{b}|^s,\boldsymbol{a}-\boldsymbol{b})\ge 2^{-s}|\boldsymbol{a}-\boldsymbol{b}|^{s+2},$$

we have

$$(|\mathcal{I}_h\boldsymbol{u}|^{r-2}\mathcal{I}_h\boldsymbol{u}-|\boldsymbol{u}_h|^{r-2}\boldsymbol{u}_h,\mathcal{I}_h\boldsymbol{u}-\boldsymbol{u}_h)\ge 2^{-(r-2)}\|\mathcal{I}_h\boldsymbol{u}-\boldsymbol{u}_h\|_{0,r}^r,$$

which implies that

$$E_{22}=-\alpha(|\mathcal{I}_h\boldsymbol{u}|^{r-2}\mathcal{I}_h\boldsymbol{u}-|\boldsymbol{u}_h|^{r-2}\boldsymbol{u}_h,\mathcal{I}_h\boldsymbol{u}-\boldsymbol{u}_h)\le 0,$$

together with the estimate of E_{21} gives that

$$E_2\le Ch^2\|\nabla\boldsymbol{\theta}\|_0. \tag{3.7}$$

Substituting the estimates of E_1-E_4 into (3.3) and applying Young's inequality leads to

$$\|\nabla\boldsymbol{\theta}\|_0^2\le Ch^4+Ch^2\|\eta\|_0. \tag{3.8}$$

On the other hand, from the discrete BB condition, we have for $\beta>0$

$$\beta\|\mathcal{J}_hp-p_h\|_0\le\sup_{0\neq\boldsymbol{v}_h\in\boldsymbol{X}_h}\frac{(\nabla\cdot\boldsymbol{v}_h,\mathcal{J}_hp-p_h)}{\|\boldsymbol{v}_h\|_1}. \tag{3.9}$$

Firstly, for $\boldsymbol{v}_h\in\boldsymbol{X}_h$, we have from Lemma 2.1, (2.6) and (3.5) that

$$\begin{aligned}
(\nabla\cdot\boldsymbol{v}_h,p-p_h)=&\nu(\nabla(\boldsymbol{u}-\boldsymbol{u}_h),\nabla\boldsymbol{v}_h)+\alpha(|\boldsymbol{u}|^{r-2}\boldsymbol{u}-|\boldsymbol{u}_h|^{r-2}\boldsymbol{u}_h,\boldsymbol{v}_h)\\
=&\nu(\nabla(\boldsymbol{u}-\mathcal{I}_h\boldsymbol{u}),\nabla\boldsymbol{v}_h)+\nu(\nabla(\mathcal{I}_h\boldsymbol{u}-\boldsymbol{u}_h),\nabla\boldsymbol{v}_h)+\alpha(|\boldsymbol{u}|^{r-2}\boldsymbol{u}-|\boldsymbol{u}_h|^{r-2}\boldsymbol{u}_h,\boldsymbol{v}_h)\\
\leq& C\nu h^2\|\boldsymbol{v}_h\|_1+C\nu\|\nabla\boldsymbol{\theta}\|_0\|\boldsymbol{v}_h\|_1+C\alpha\int_\Omega(|\boldsymbol{u}|+|\boldsymbol{u}_h|)^{r-2}|\boldsymbol{u}-\boldsymbol{u}_h||\boldsymbol{v}_h|dxdy\\
\leq& C\nu h^2\|\boldsymbol{v}_h\|_1+C\nu\|\nabla\boldsymbol{\theta}\|_0\|\boldsymbol{v}_h\|_1\\
&+C\alpha\left(\int_\Omega\left[(|\boldsymbol{u}|+|\boldsymbol{u}_h|)^{r-2}\right]^{r'}dxdy\right)^{\frac{1}{r'}}\left(\int_\Omega|\boldsymbol{u}-\boldsymbol{u}_h|^r dxdy\right)^{\frac{1}{r}}\left(\int_\Omega|\boldsymbol{v}_h|^r dxdy\right)^{\frac{1}{r}}\\
\leq& C\nu h^2\|\boldsymbol{v}_h\|_1+C\nu\|\nabla\boldsymbol{\theta}\|_0\|\boldsymbol{v}_h\|_1+C\alpha(\|\boldsymbol{u}\|_{0,r}+\|\boldsymbol{u}_h\|_{0,r})^{r-2}\|\boldsymbol{u}-\boldsymbol{u}_h\|_{0,r}\|\boldsymbol{v}_h\|_{0,r}\\
\leq& C\nu h^2\|\boldsymbol{v}_h\|_1+C\nu\|\nabla\boldsymbol{\theta}\|_0\|\boldsymbol{v}_h\|_1+C\alpha(\|\boldsymbol{u}\|_{0,r}+\|\boldsymbol{u}_h\|_{0,r})^{r-2}(h^2+\|\nabla\boldsymbol{\theta}\|_0)\|\boldsymbol{v}_h\|_1\\
\leq& C(\nu+\alpha(\|\boldsymbol{u}\|_{0,r}+\|\boldsymbol{u}_h\|_{0,r})^{r-2}))h^2\|\boldsymbol{v}_h\|_1\\
&+C(\nu+\alpha(\|\boldsymbol{u}\|_{0,r}+\|\boldsymbol{u}_h\|_{0,r})^{r-2})\|\nabla\boldsymbol{\theta}\|_0\|\boldsymbol{v}_h\|_1\\
\leq& Ch^2\|\boldsymbol{v}_h\|_1+C\|\nabla\boldsymbol{\theta}\|_0\|\boldsymbol{v}_h\|_1,
\end{aligned}\tag{3.10}$$

where $\frac{1}{r'}+\frac{2}{r}=1$ and we have used interpolation theory and $H^1(\Omega)\hookrightarrow L^r(\Omega)$.

Secondly, from Lemma 2.2, it follows that

$$(\nabla\cdot\boldsymbol{v}_h,p-\mathcal{J}_hp)\leq Ch^2\|p\|_2\|\boldsymbol{v}_h\|_1.\tag{3.11}$$

Thus, we have from (3.10) and (3.11)

$$\begin{aligned}
(\nabla\cdot\boldsymbol{v}_h,\mathcal{J}_hp-p_h)=&(\nabla\cdot\boldsymbol{v}_h,\mathcal{J}_hp-p)+(\nabla\cdot\boldsymbol{v}_h,p-p_h)\\
\leq& Ch^2\|\boldsymbol{v}_h\|_1+C\|\nabla\boldsymbol{\theta}\|_0\|\boldsymbol{v}_h\|_1.
\end{aligned}\tag{3.12}$$

Substituting (3.12) and (3.8) into (3.9) gives

$$\|\mathcal{J}_hp-p_h\|_0\leq Ch^2+Ch\|\mathcal{J}_hp-p_h\|_0^{\frac{1}{2}},\tag{3.13}$$

which shows that by applying Young's inequality

$$\|\mathcal{J}_hp-p_h\|_0\leq Ch^2.\tag{3.14}$$

Taking the above estimate (3.14) into (3.8) implies that

$$\|\nabla(\mathcal{I}_h\boldsymbol{u}-\boldsymbol{u}_h)\|_0\leq Ch^2.\tag{3.15}$$

By Poincáre inequality, there holds $\|\mathcal{I}_h\boldsymbol{u}-\boldsymbol{u}_h\|_1\leq Ch^2$. The proof is completed. □

Remark 3.1. By triangular inequality and interpolation theory [28], the following optimal error estimate holds

$$\|\boldsymbol{u}-\boldsymbol{u}_h\|_1+\|p-p_h\|_0\leq Ch.$$

In order to obtain global superconvergence result, we introduce two postprocessing operators [24]. For the velocity, we define $\mathcal{I}_{2h}$ as the piecewise biquadratic Lagrange interpolation operator associated with $\mathcal{T}_{2h}$. For the pressure, we define $\mathcal{J}_{2h}$ as

$$\mathcal{J}_{2h}p\in Q_{11}(\tau), \quad \int_{e_i}(\mathcal{J}_{2h}p-p)dxdy=0, \quad i=1,2,3,4,$$

where $Q_{11}(\tau)$ denotes the space of all polynomials defined on τ of degree ≤ 1 with respect to each of the two variables x and y.

The following properties have been shown in [24]:

$$\left\{\begin{array}{l}\mathcal{I}_{2h}\mathcal{I}_h=\mathcal{I}_{2h},\\ \|\mathcal{I}_{2h}\boldsymbol{v}\|_1\leq C\|\boldsymbol{v}\|_1, \quad \forall \boldsymbol{v}\in \boldsymbol{X}_h,\\ \|\boldsymbol{u}-\mathcal{I}_{2h}\boldsymbol{u}\|_1\leq Ch^2\|\boldsymbol{u}\|_3,\end{array}\right. \qquad \left\{\begin{array}{l}\mathcal{J}_{2h}\mathcal{J}_h=\mathcal{J}_{2h},\\ \|\mathcal{J}_{2h}q\|_0\leq C\|q\|_0, \quad \forall q\in P_h,\\ \|p-\mathcal{J}_{2h}p\|_0\leq Ch^2\|p\|_2.\end{array}\right. \tag{3.16}$$

Then, we give the global superconvergence results for velocity $\boldsymbol{u}$ and pressure p in the following theorem.

Theorem 3.2. *Suppose all conditions of Theorem* 3.1 *are valid. Then*

$$\|\boldsymbol{u}-\mathcal{I}_{2h}\boldsymbol{u}_h\|_1+\|p-\mathcal{J}_{2h}p_h\|_0\leq Ch^2. \tag{3.17}$$

Proof. From the property (3.16), Theorem 3.1, we have

$$\begin{aligned}&\|\boldsymbol{u}-\mathcal{I}_{2h}\boldsymbol{u}_h\|_1+\|p-\mathcal{J}_{2h}p_h\|_0\\ \leq&\|\mathcal{I}_{2h}(\boldsymbol{u}_h-\mathcal{I}_h\boldsymbol{u})\|_1+\|\boldsymbol{u}-\mathcal{I}_{2h}\mathcal{I}_h\boldsymbol{u}\|_1+\|\mathcal{J}_{2h}(p_h-\mathcal{J}_hp)\|_0+\|p-\mathcal{J}_{2h}\mathcal{J}_hp\|_0\\ \leq&C\|\boldsymbol{u}_h-\mathcal{I}_h\boldsymbol{u}\|_1+Ch^2\|\boldsymbol{u}\|_3+C\|p_h-\mathcal{J}_hp\|_0+Ch^2\|p\|_2\leq Ch^2.\end{aligned}$$

The proof is completed. $\square$

4 Numerical experiment

Since the system is nonlinear, we use the Picard iteration to solve the nonlinear system and present it as follows:

Step 1. Take the initial value $(\boldsymbol{u}_h^0,p_h^0)\in \boldsymbol{X}_h\times P_h$, such that

$$\left\{\begin{array}{ll}a_0(\boldsymbol{u}_h^0,\boldsymbol{v}_h)-b(\boldsymbol{v}_h,p_h^0)=(\boldsymbol{f},\boldsymbol{v}_h), & \forall \boldsymbol{v}_h\in \boldsymbol{X}_h,\\ b(\boldsymbol{u}_h^0,q_h)=0, & \forall q_h\in P_h.\end{array}\right.$$

Step 2. For $\ell\geq 0$, compute $(\boldsymbol{u}_h^{\ell+1},p_h^{\ell+1})\in \boldsymbol{X}_h\times P_h$, such that

$$\left\{\begin{array}{ll}a_0(\boldsymbol{u}_h^{\ell+1},\boldsymbol{v}_h)+a_1(\boldsymbol{u}_h^{\ell};\boldsymbol{u}_h^{\ell+1},\boldsymbol{v}_h)-b(\boldsymbol{v}_h,p_h^{\ell+1})=(\boldsymbol{f},\boldsymbol{v}_h), & \forall \boldsymbol{v}_h\in \boldsymbol{X}_h,\\ b(\boldsymbol{u}_h^{\ell+1},q_h)=0, & \forall q_h\in P_h.\end{array}\right.$$

Step 3. For a fixed tolerance ε, stop the iteration if

$$\|\boldsymbol{u}-\boldsymbol{u}_h\|_1 \leq \varepsilon.$$

Otherwise, set $\ell \leftarrow \ell+1$ and go to Step 2 to continue the nonlinear iteration.

Let $\Omega=(0,1)\times(0,1)$ and divide Ω into $m\times n$ uniform rectangles with $m\times n=8\times 8$, 16×16, 32×32, 64×64, respectively.

Example 4.1. The source term $\boldsymbol{f}$ and the boundary condition are chosen corresponding to the exact solution (cf. [5,6]):

$$\begin{aligned}&u_1=-\sin^2(\pi x)\sin(\pi y)\cos(\pi y), \quad u_2=\sin(\pi x)\cos(\pi x)\sin^2(\pi y),\\ &p=\sin(\pi x)\cos(\pi y).\end{aligned}$$

The numerical errors of the velocity $\boldsymbol{u}$ and the pressure p with $\nu=1$, $\alpha=1e-2$, $r=3$ are listed in Tables 1-2. Obviously, from Tables 1-2, it can be seen that numerical results are in agreement with the theoretical analysis, i.e., the convergence rates of $\|\boldsymbol{u}-\boldsymbol{u}_h\|_1$, $\|\mathcal{I}_h\boldsymbol{u}-\boldsymbol{u}_h\|_1$, $\|\boldsymbol{u}-\mathcal{I}_{2h}\boldsymbol{u}_h\|_1$ and $\|p-p_h\|_0$, $\|\mathcal{J}_h p-p_h\|_0$, $\|p-\mathcal{J}_{2h}p_h\|_0$ are $\mathcal{O}(h)$, $\mathcal{O}(h^2)$ and $\mathcal{O}(h^2)$, respectively. At the same time, we also give the graphics of the exact solutions $(u,\boldsymbol{p})$ and finite element solutions $(u_h, \boldsymbol{p}_h)$ on mesh 64×64 (see Fig. 3), which also shows that the numerical solutions approximate the exact solutions very well.

Table 1: The errors of $\boldsymbol{u}$ with $\nu=1$, $\alpha=1e-2$, $r=3$.

$m\times n$	8×8	16×16	32×32	64×64
$\|\boldsymbol{u}-\boldsymbol{u}_h\|_1$	5.0290e-01	2.5173e-01	1.2590e-01	6.2956e-02
Order	/	0.99838	0.99959	0.99990
$\|\mathcal{I}_h\boldsymbol{u}-\boldsymbol{u}_h\|_1$	5.3255e-02	1.4239e-02	3.6183e-03	9.0825e-04
Order	/	1.9031	1.9764	1.9942
$\|\boldsymbol{u}-\mathcal{I}_{2h}\boldsymbol{u}_h\|_1$	2.0713e-01	5.2792e-02	1.3256e-02	3.3176e-03
Order	/	1.9722	1.9936	1.9985

Table 2: The errors of p with $\nu=1$, $\alpha=1e-2$, $r=3$.

$m\times n$	8×8	16×16	32×32	64×64
$\|p-p_h\|_0$	8.9153e-02	4.1331e-02	2.0200e-02	1.0040e-02
Order	/	1.1091	1.0328	1.0086
$\|\mathcal{J}_h p-p_h\|_0$	3.9957e-02	1.0318e-02	2.5976e-03	6.5049e-04
Order	/	1.9532	1.9900	1.9976
$\|p-\mathcal{J}_{2h}p_h\|_0$	4.6426e-02	1.1302e-02	2.8029e-03	6.9917e-04
Order	/	2.0383	2.0116	2.0032

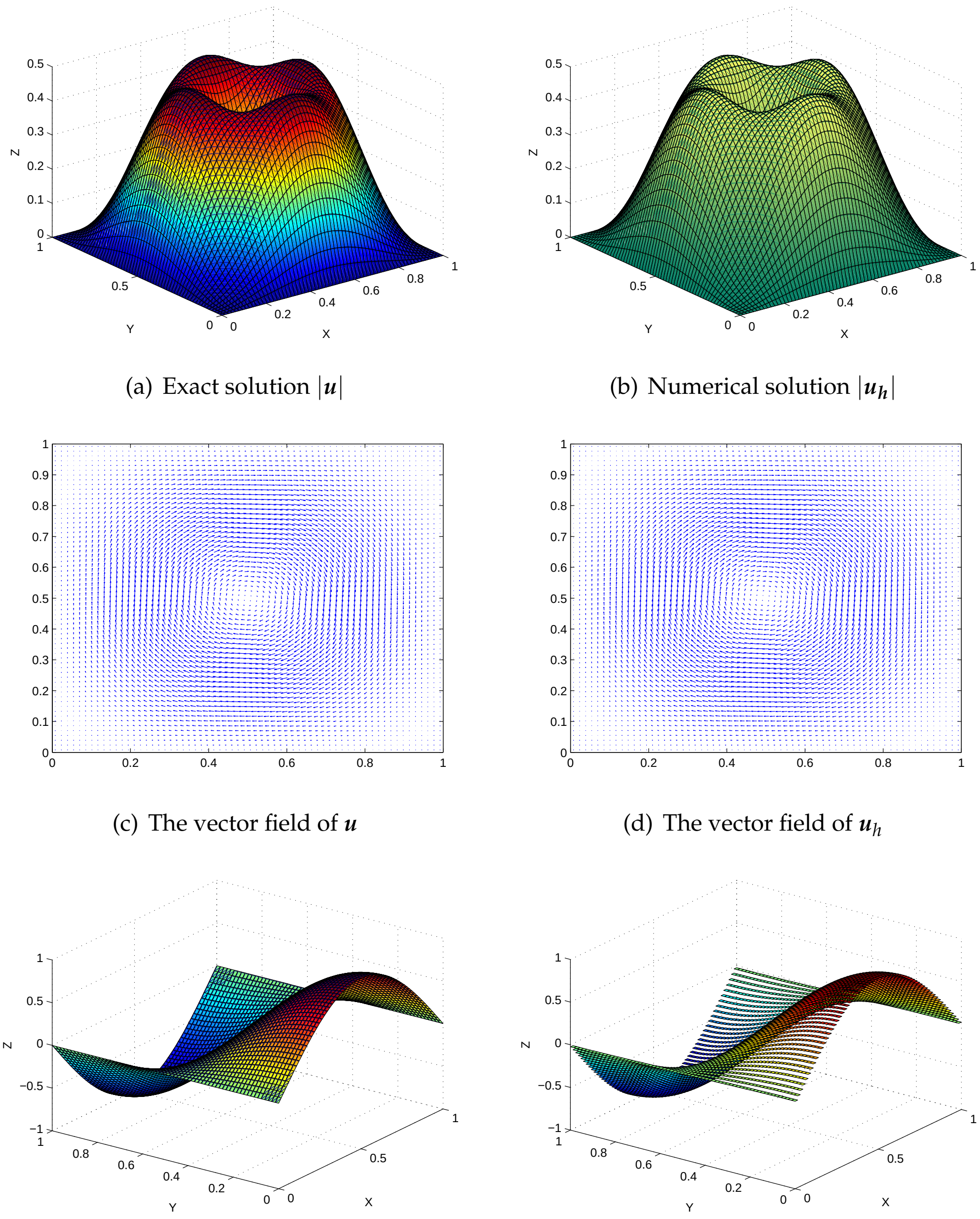

(a) Exact solution $|\boldsymbol{u}|$ (b) Numerical solution $|\boldsymbol{u_h}|$

(c) The vector field of $\boldsymbol{u}$ (d) The vector field of $\boldsymbol{u}_h$

(e) Exact solution p (f) Numerical solution p_h

Figure 3: The graphics on 64×64 with $\nu=1$, $\alpha=1e-2$, $r=3$ of Example 4.1.

Example 4.2. The source term $\boldsymbol{f}$ and the boundary condition are chosen corresponding to the exact solution (cf. [29]):

$$u_1=(x^4-2x^3+x^2)(4y^3-6y^2+2y),\quad u_2=-(y^4-2y^3+y^2)(4x^3-6x^2+2x),$$
$$p=10(2x-1)(2y-1).$$

The numerical errors of the velocity $\boldsymbol{u}$ and the pressure p with $\nu=0.01$, $\alpha=10$, $r=2.9$ are listed in Tables 3-4. Obviously, from Tables 3-4, it can be seen that numerical results are in agreement with the theoretical analysis i.e., the convergence rates of $\|\boldsymbol{u}-\boldsymbol{u}_h\|_1$, $\|\mathcal{I}_h\boldsymbol{u}-\boldsymbol{u}_h\|_1$, $\|\boldsymbol{u}-\mathcal{I}_{2h}\boldsymbol{u}_h\|_1$ and $\|p-p_h\|_0$, $\|\mathcal{J}_hp-p_h\|_0$, $\|p-\mathcal{J}_{2h}p_h\|_0$ are $\mathcal{O}(h)$, $\mathcal{O}(h^2)$ and $\mathcal{O}(h^2)$, respectively. At the same time, we also give the graphics of the exact solutions (u, $\boldsymbol{p}$) and finite element solutions (u_h, $\boldsymbol{p}_h$) on mesh 64×64 (see Fig. 4), which also shows that the numerical solutions approximate the exact solutions very well.

Table 3: The errors of $\boldsymbol{u}$ with $\nu=0.01$, $\alpha=10$, $r=2.9$.

$m\times n$	8×8	16×16	32×32	64×64
$\|\boldsymbol{u}-\boldsymbol{u}_h\|_1$	1.5418e-02	7.7142e-03	3.8575e-03	1.9288e-03
Order	/	0.99900	0.99986	0.99997
$\|\mathcal{I}_h\boldsymbol{u}-\boldsymbol{u}_h\|_1$	2.4346e-03	6.4244e-04	1.6272e-04	4.0812e-05
Order	/	1.9221	1.9812	1.9953
$\|\boldsymbol{u}-\mathcal{I}_{2h}\boldsymbol{u}_h\|_1$	5.1951e-03	1.2945e-003	3.2304e-04	8.0719e-05
Order	/	2.0047	2.0026	2.0007

Table 4: The errors of p with $\nu=0.01$, $\alpha=10$, $r=2.9$.

$m\times n$	8×8	16×16	32×32	64×64
$\|p-p_h\|_0$	6.0739e-01	2.9692e-01	1.4760e-01	7.3693e-02
Order	/	1.0325	1.0084	1.0021
$\|\mathcal{J}_hp-p_h\|_0$	1.5625e-01	3.9063e-02	9.7656e-03	2.4414e-03
Order	/	2.0000	2.0000	2.0000
$\|p-\mathcal{J}_{2h}p_h\|_0$	2.0833e-01	5.2083e-02	1.3021e-02	3.2552e-03
Order	/	2.0000	2.0000	2.0000

Example 4.3. In this example, we consider a lid-driven cavity flow problem [4]. In this problem, a unit velocity is specified along the entire top surface and zero velocity on the other surfaces as shown in Fig. 5.

We consider the flow for fixed parameters $\nu=0.01$, $r=2.9$ and $h=1/64$ as [4] and take $\alpha=0.1$, 0, 1 and 10, respectively. We present the streamline pattern in Fig. 6, which shows that the results obtained herein are in good agreement with the phenomenon discussed in [4].

On the other hand, we also consider the flow for fixed parameters $\alpha=100$, $r=2.9$ and $h=1/64$ as [4] and take $\nu=0.001$, 0.01, 0.1 and 1, respectively. We present the streamline pattern in Fig. 7, which shows that the effect of damping term increases with the decrease of viscosity.

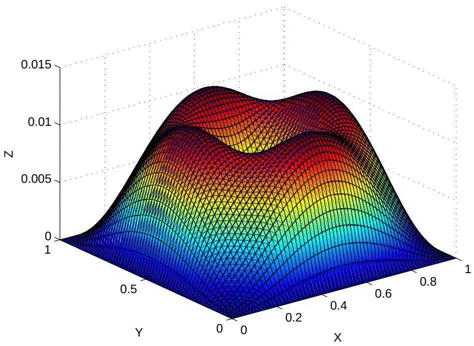

(a) Exact solution $|\boldsymbol{u}|$

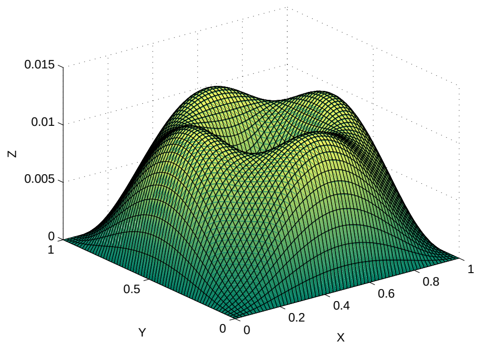

(b) Numerical solution $|\boldsymbol{u_h}|$

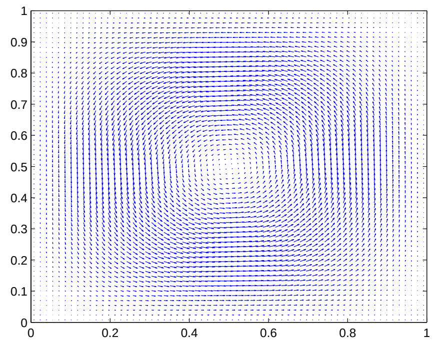

(c) The vector field of $\boldsymbol{u}$

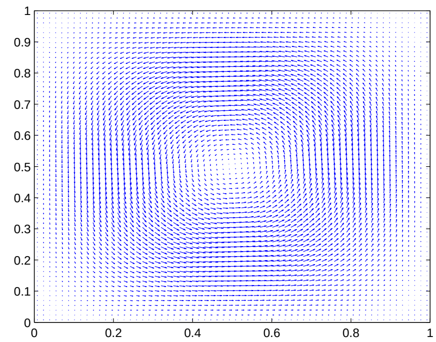

(d) The vector field of $\boldsymbol{u}_h$

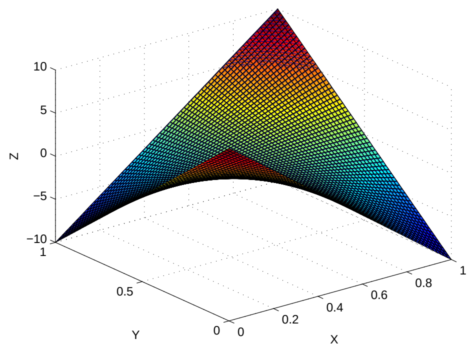

(e) Exact solution p

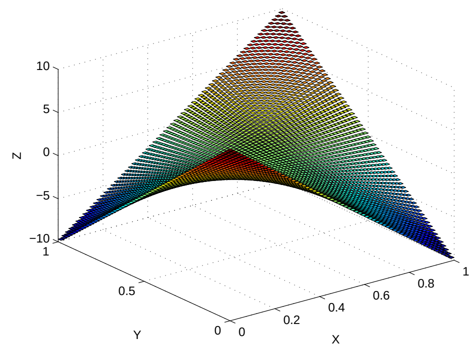

(f) Numerical solution p_h

Figure 4: The graphics on 64×64 with $\nu=0.01$, $\alpha=10$, $r=2.9$ of Example 4.2.

5 Conclusions

In this work, the superconvergence error analysis is investigated for the Stokes equations with a low order conforming mixed finite element method (called bilinear-constant

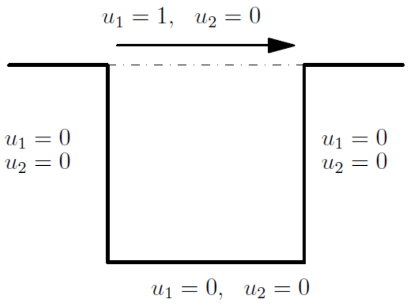

Figure 5: Model description of Example 4.3.

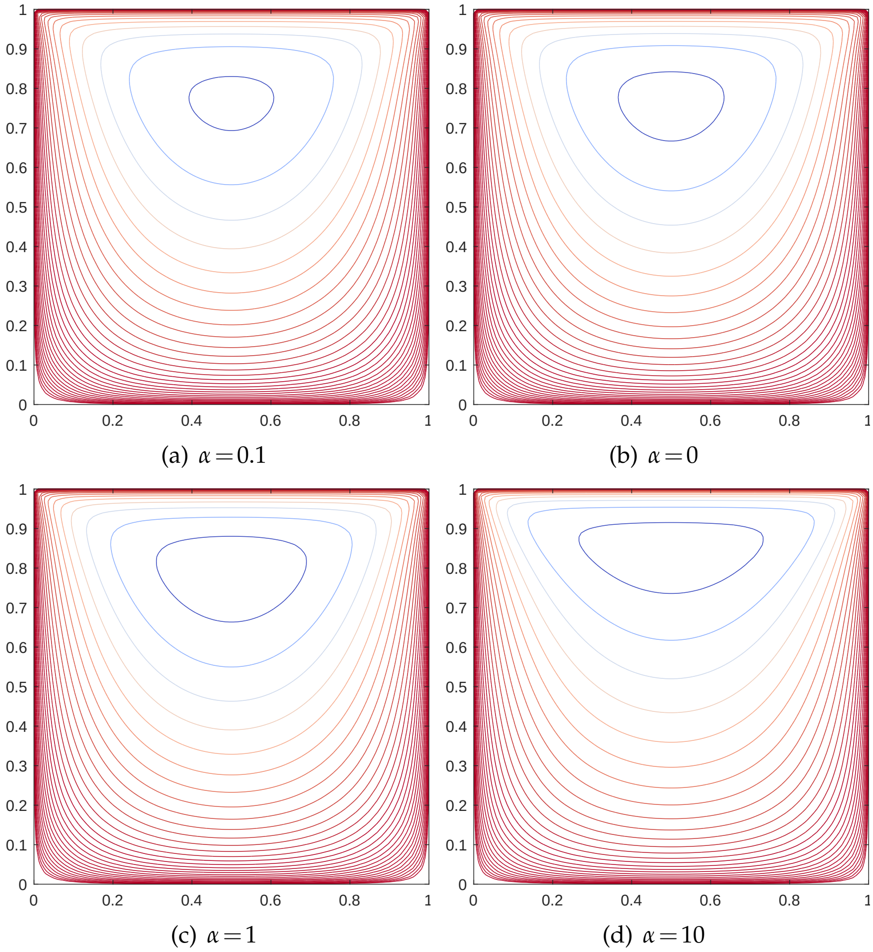

Figure 6: The streamline pattern with $\nu=0.01$, $r=2.9$, $h=1/64$ and different α.

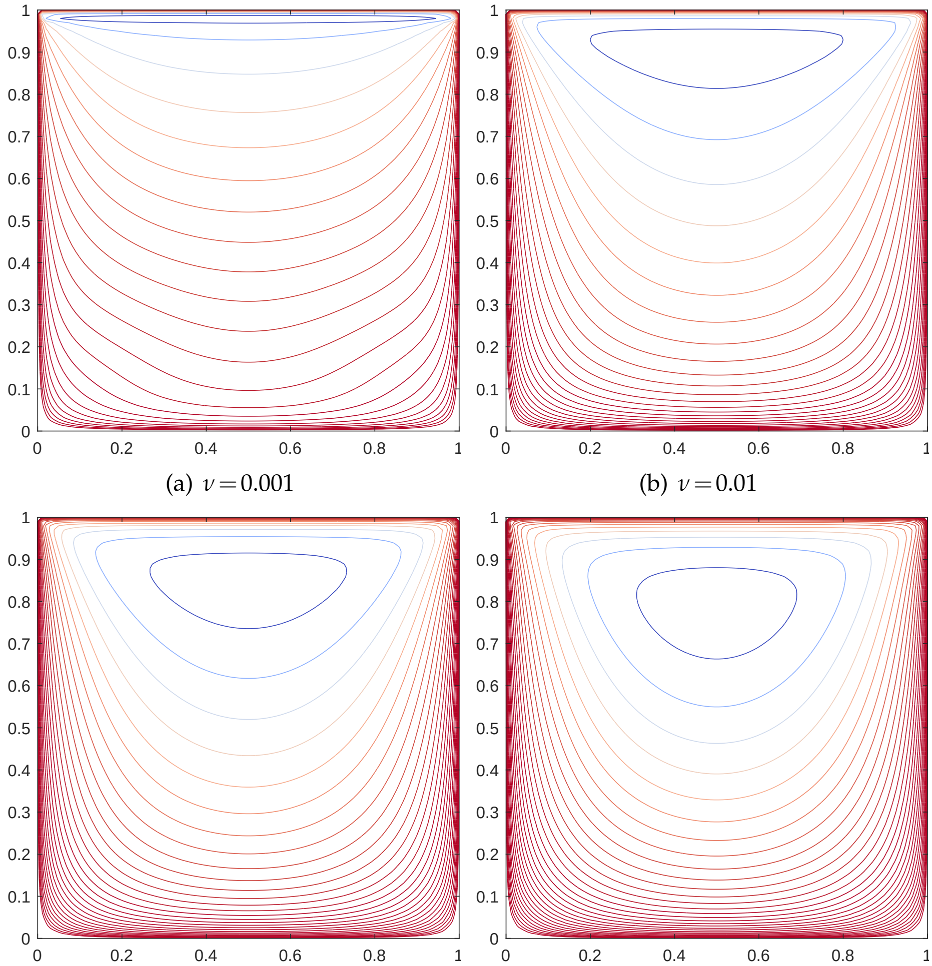

(a) $\nu=0.001$ (b) $\nu=0.01$

(c) $\nu=0.1$ (d) $\nu=1$

Figure 7: The streamline pattern with $\alpha=100$, $r=2.9$, $h=1/64$ and different ν.

scheme [24]). The error analysis is divided into two parts. In the first part, with the help of the integral identity technique [11,12,24,25] and treating the damping term carefully and skillfully, the superclose error estimates for the velocity in H^1-norm and the pressure in L^2-norm are derived. Subsequently, in the second part, according to the interpolation postprocessing approach, the global superconvergence results for the velocity in H^1-norm and the pressure in L^2-norm are obtained effectively. Moreover, some numerical experiments are carried out to support the theoretical analysis. In the future work, we will focus on the numerical approximations for the time-dependent Navier-Stokes/Stokes equations with damping by using low order conforming/nonconforming mixed finite element methods.

Acknowledgements

This work was supported by National Natural Science Foundation of China (No. 12101568) and the Doctoral Starting Foundation of Zhengzhou University of Aeronautics (No. 63020390).

References

[1] P. FORCHHEIMER, *Wasserbewegung durch Boden,* Z. Ver. Dtsch. Ing., 45 (1901), pp. 1782–1788.

[2] D. BRESCH, AND B. DESJARDINS, *Existence of global weak solutions for a 2D viscous shallow water equations and convergence to the quasi-geostrophic model,* Commun. Math. Phys., 238(1-2) (2003), pp. 211–223.

[3] D. BRESCH, B. DESJARDINS, AND C. K. LIN, *On some compressible fluid models: Korteweg, lubrication, and shallow water systems,* Commun. Partial Differential Equations, 28(3-4) (2003), pp. 843–868.

[4] D. M. LIU, AND K. T. LI, *Finite element analysis of the Stokes equations with damping,* Math. Numer. Sin., 32(4) (2010), pp. 433–448.

[5] M. H. LI, D. Y. SHI, AND Y. DAI, *Stabilized low order finite elements for Stokes equations with damping,* J. Math. Anal. Appl., 435 (2016), pp. 646–660.

[6] Y. SUN, AND H. X. RUI, *MAC finite difference scheme for Stokes equations with damping on non-uniform grids,* Comput. Math. Appl., 75 (2018), pp. 1272–1287.

[7] D. Y. SHI, AND Z. Y. YU, *Superclose and superconvergence of finite element discretizations for the Stokes equations with damping,* Appl. Math. Comput., 213 (2013), pp. 7693–7698.

[8] X. CAI, AND Q. JIU, *Weak and strong solutions for the incompressible Navier-Stokes equations with damping,* J. Math. Anal. Appl., 343(2) (2008), pp. 799–809.

[9] X. X. DING, AND Y. H. WU, *Finite dimensional behaviors of Navier-Stokes equations with linear dampness on the whole R^2 space,* Acta Math. Appl. Sin., 20(4) (1997), pp. 509–520.

[10] C. S. ZHAO, AND K. T. LI, *The global attractor of Navier-Stokes equations with linear dampness on the whole two-dimensional space and estimates of its dimensions,* Acta Math. Appl. Sin., 23(1) (2000), pp. 90–98.

[11] Q. LIN, AND J. F. LIN, Finite Element Methods: Accuracy and Improvement, Science Press, Beijing, 2006.

[12] N. YAN, Superconvergence Analysis and a Posteriori Error Estimation in Finite Element Methods, Science Press, 2008.

[13] Q. LIN. L. TOBISKA, AND A. H. ZHOU, *Superconvergence and extrapolation of nonconforming low order finite elements applied to the poisson equation,* IMA J. Numer. Anal., 25 (2005), pp. 160–181.

[14] Y. M. ZHAO, P. CHEN, W. P. BU, X. T. LIU, AND Y. F. TANG, *Two mixed finite element methods for time-fractional difusion equations,* J. Sci. Comput., 70(1) (2017), pp. 407–428.

[15] M. LI, Q. LIN, AND S. ZHANG, *Extrapolation and supercnvergence of the Steklov eigenvalue problem,* Adv. Comput. Math., 33 (2010), pp. 25–44.

[16] Y. Q. HUANG, J. C. LI, AND W. YANG, *Superconvergence analysis for linear tetrahedral edge elements,* J. Sci. Comput., 62 (2015), pp. 122–145.

[17] M. SUN, J. C. LI, P. Z. WANG, AND Z. M. ZHANG, *Superconvergence analysis of high-order rectangular edge elements for time-harmonic Maxwell's equations,* J. Sci. Comput., 75(1) (2018), pp. 510–535.

[18] D. Y. SHI, AND J. J. WANG, *Unconditional superconvergence analysis of a Crank-Nicolson Galerkin FEM for nonlinear Schrödinger equation,* J. Sci. Comput., 72(3) (2017), pp. 1093–1118.

[19] D. Y. SHI, AND H. J. YANG, *Superconvergent estimates of conforming finite element method for nonlinear time-dependent Joule heating equations,* Numer. Methods Partial Differential Equations, 34(1) (2018), pp. 336–356.

[20] D. Y. SHI, AND H. J. YANG, *Superconvergence analysis of finite element method for Poisson-Nernst-Planck equations,* Numer. Methods Partial Differential Equations, 35(3) (2019), pp. 1206–1223.

[21] H. H. XIE, *Extrapolation of Nédélec element for the Maxwell equations by the mixed finite element method,* Adv, Coput. Math., 29(2) (2008), pp. 135–145.

[22] H. P. LIU, AND N. N. YAN, *Superconvergence analysis of the nonconforming quadrilatral linear-constant scheme for Stokes equations,* Adv. Comput. Math., 29(4) (2008), pp. 375–392.

[23] J. C. REN, AND Y. MA, *A superconvergent nonconforming mixed finite element method for the Navier-Stokes equations,* Numer. Methods Partial Differential Equations, 32(2) (2016), pp. 646–660.

[24] J. H. PAN, *Global superconvergence for the bilinear-constant scheme for the Stokes problem,* SIAM J. Numer. Anal., 36(6) (1997), pp. 2424–2430.

[25] H. P. LIU, AND N. N. YAN, *Global superconvergence for optimal control problems governed by Stokes equations,* Int. J. Numer. Anal. Model., 3(3) (2006), pp. 283-302.

[26] R. A. ADAMS, AND J. J. F. FOURNIER, Sobolev Spaces, Academic press, 2003.

[27] V. GIRAULT, AND P. RAVIART, Finite Element Methods for Navier-Stokes Equations. Theory and Algorithms, Springer-Verlag, Heidelberg, 1986.

[28] S. C. BRENNER, AND L. R. SCOTT, The Mathematical Theory of Finite Element Methods, Springer-Verlag, New York, 2008.

[29] C. XU, D. Y. SHI, AND X. LIAO, *Low order nonconforming mixed finite element method for non-stationary incompressible Navier-Stokes equations,* Appl. Math. Meth. Eng., 37(18) (2016), pp. 1095–1112.